iScience

CellPress
OPEN ACCESS

Article

# A host lipase prevents lipopolysaccharide-induced foam cell formation

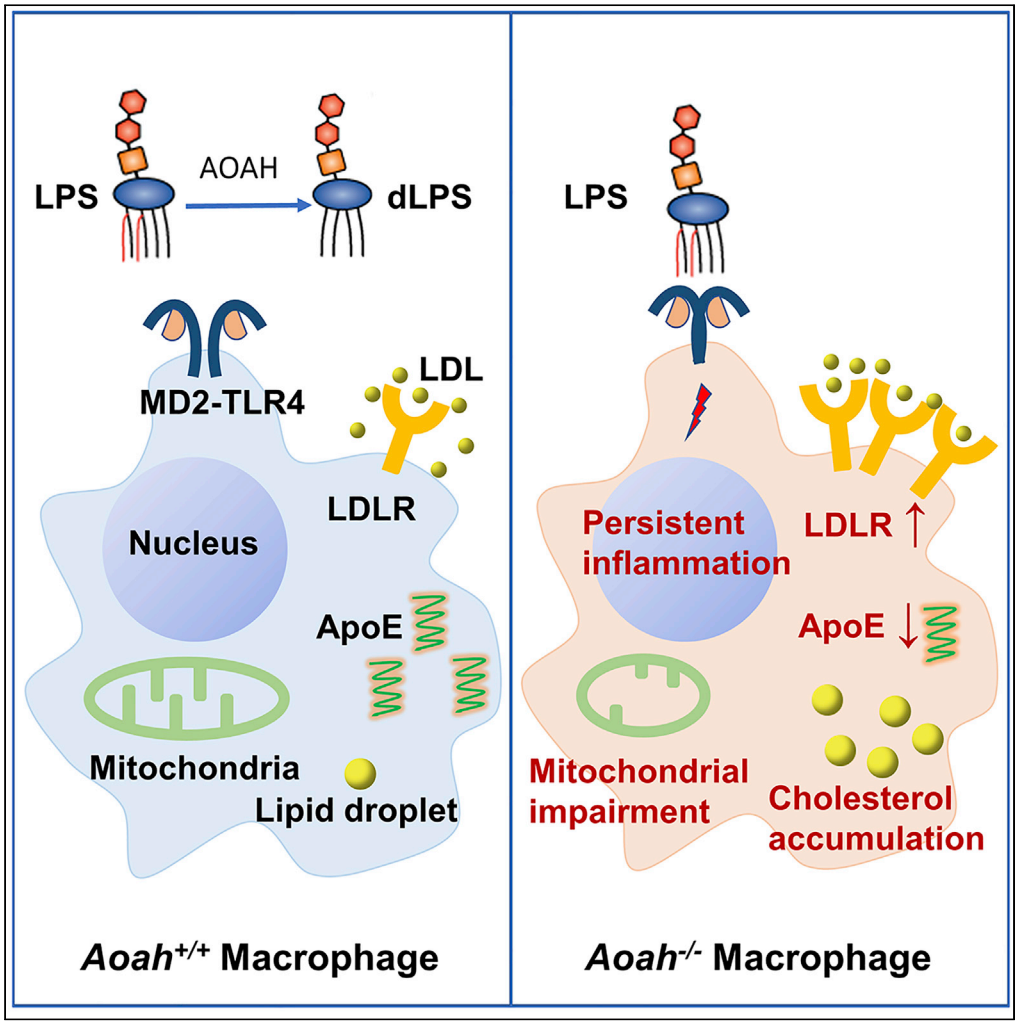


Jintao Feng, Wei Jiang, Xiaofang Cheng, ..., Xiaobo Li, Robert S. Munford, Mingfang Lu

mingfanglu@fudan.edu.cn

## Highlights

Acyloxyacyl hydrolase prevents LPS-induced cholesterol accumulation in macrophages

AOAH also prevents prolonged inflammation after LPS exposure

AOAH enhances mitochondrial function in LPS-exposed macrophages

AOAH ameliorates LPS-induced foam cell accumulation in carotid arterial lesions

Feng et al., iScience 24, 103004
September 24, 2021 
https://doi.org/10.1016/j.isci.2021.103004

iScience

CellPress
OPEN ACCESS

Article

# A host lipase prevents lipopolysaccharide-induced foam cell formation

Jintao Feng,[1,8] Wei Jiang,[1,2,8] Xiaofang Cheng,[1,8] Benkun Zou,[1] Alan W. Varley,[3] Ting Liu,[1] Guojun Qian,[1] Wenjiao Zeng,[4] Jianguo Tang,[2] Qiang Zhao,[5] Yiwei Chu,[1] Yuanyuan Wei,[1] Xiaobo Li,[6] Robert S. Munford,[7] and Mingfang Lu[1,2,9,*]

## SUMMARY

**Although microbe-associated molecular pattern (MAMP) molecules can promote cholesterol accumulation in macrophages, the existence of a host-derived MAMP inactivation mechanism that prevents foam cell formation has not been described. Here, we tested the ability of acyloxyacyl hydrolase (AOAH), the host lipase that inactivates gram-negative bacterial lipopolysaccharides (LPSs), to prevent foam cell formation in mice. Following exposure to small intraperitoneal dose(s) of LPSs, *Aoah*$^{-/-}$ macrophages produced more low-density lipoprotein receptor and less apolipoprotein E and accumulated more cholesterol than did *Aoah*$^{+/+}$ macrophages. The *Aoah*$^{-/-}$ macrophages also maintained several pro-inflammatory features. Using a perivascular collar placement model, we found that *Aoah*$^{-/-}$ mice developed more carotid artery foam cells than did *Aoah*$^{+/+}$ mice after they had been fed a high fat, high cholesterol diet, and received small doses of LPSs. This is the first demonstration that an enzyme that inactivates a stimulatory MAMP *in vivo* can reduce cholesterol accumulation and inflammation in arterial macrophages.**

## INTRODUCTION

Much evidence supports the hypothesis that microbe-associated molecular pattern (MAMP) stimulation of Toll-like receptor (TLR) signaling can promote lipid accumulation in macrophages and contribute to the pathogenesis of atherosclerosis (Curtiss and Tobias, 2009; Bjorkbacka et al., 2004; Nicolaou and Erridge, 2010; Nicolaou et al., 2012; Vink et al., 2002; Angelovich et al., 2015; Zimmer et al., 2015; Hsieh et al., 2020) while defective resolution of inflammatory changes in macrophages may be exacerbating (Tabas, 2010; Back et al., 2019). Lipopolysaccharide (LPS, endotoxin), a major component of the gram-negative bacterial outer membrane, can be a potent MAMP, stimulating macrophages to induce innate responses that promote inflammation. Previous studies have found that experimental endotoxemia can drive sustained monocyte inflammation and atherosclerosis in mice (Geng et al., 2016; Stoll et al., 2004; Lu et al., 2017). In addition, the severity of atherosclerosis was significantly reduced in mice that lacked the LPS receptor TLR4 or a downstream signaling molecule, MyD88 (Bjorkbacka et al., 2004; Michelsen et al., 2004).

Acyloxyacyl hydrolase (AOAH) is a highly conserved host lipase that is mainly produced by monocyte-macrophages, neutrophils, and NK cells (reviewed in (Munford et al., 2020)). AOAH inactivates LPS by cleaving secondary fatty acyl chains from the diglucosamine backbone of lipid A; the resulting tetraacyl LPS is non-stimulatory and may inhibit LPS signaling. Enzymatic deacylation of LPS may occur either intracellularly in endosome-lysosomes or extracellularly, where the enzyme's ability to act on LPS can be greatly enhanced by LPS-binding protein and soluble CD14 (Gioannini et al., 2007). Previous studies have found that AOAH enables recovery from endotoxin tolerance (Lu et al., 2008, 2013), limits LPS-induced B-cell activation and innate antibody production (Lu et al., 2005), deacylates LPS in a local tissue site before the LPS is carried by lymphatics to regional nodes or blood (Lu and Munford, 2011), inactivates LPS that translocates from the small intestine into the portal vein (Han et al., 2021), accelerates resolution of LPS-induced inflammation (Zou et al., 2017), and sensitizes lung epithelial cells for allergic asthma by degrading intestinal commensal LPSs (Qian et al., 2018). Although numerous other host mechanisms for inactivating LPSs have been described, none has compensated for the absence of AOAH in these murine models (Munford et al., 2020).

[1]Department of Immunology, Key Laboratory of Medical Molecular Virology (MOE, NHC, CAMS), School of Basic Medical Sciences, Fudan University, Shanghai 200032, China

[2]Department of Trauma-Emergency & Critical Care Medicine, Shanghai Fifth People's Hospital, Fudan University, Shanghai 200040, China

[3]Department of Internal Medicine, UT-Southwestern Medical Center at Dallas, Texas 75390, USA

[4]Department of Pathology, School of Basic Medical Sciences, Fudan University, Shanghai 200032, China

[5]Department of Cardiac Surgery, Ruijin Hospital, Shanghai Jiao Tong University School of Medicine, Shanghai 200020, China

[6]Department of Physiology and Pathophysiology, School of Basic Medical Sciences, Fudan University, Shanghai 200032, China

[7]Antibacterial Host Defense Unit, Laboratory of Clinical Immunology and Microbiology, National Institute of Allergy and Infectious Diseases (NIAID), National Institutes of Health (NIH), Bethesda, MD 20892, USA

[8]These authors contributed equally

[9]Lead contact

*Correspondence: mingfanglu@fudan.edu.cn

https://doi.org/10.1016/j.isci.2021.103004

Intrigued by reports that (a) endotoxemia may be associated with carotid atherosclerosis and cardiovascular disease in humans (Wiedermann et al., 1999), (b) *E. coli* LPSs may be found in human carotid atheromata (Carnevale et al., 2018), (c) intronic *Aoah* single nucleotide polymorphisms (SNPs) may be associated with carotid bifurcation intima-media thickness in humans (Wang et al., 2015), and (d) low-grade endotoxemia promotes atherosclerosis in mice while a TLR4 antagonist or the absence of TLR4 can prevent it (Vink et al., 2002; Geng et al., 2016; Stoll et al., 2004; Michelsen et al., 2004; Lu et al., 2017); we tested the hypothesis that AOAH prevents foam cell formation in murine macrophages when they are exposed to LPS. Attempting to mimic natural exposure more closely, we used *in vivo* LPS doses that were lower than those shown to produce atherosclerosis in most previous studies (Westerterp et al., 2007; Malik et al., 2010; Gitlin and Loftin, 2009; Lu et al., 2017).

## RESULTS

### LPS-exposed *Aoah*$^{-/-}$ peritoneal macrophages accumulate more cholesterol

In preliminary experiments, we confirmed that approximately 75% of the macrophages isolated from peritoneal fluid two weeks after intraperitoneally (i.p.) LPS injection were derived from recruited monocytes (Figures S1A and S1B) (Ghosn et al., 2010). We considered these cells to be representative of recruited monocyte-macrophages in other tissues, including arterial lesions (Moore et al., 2013; Williams et al., 2020). The inflammatory impact of an intraperitoneal dose of LPS lasts only a few days in *Aoah*$^{+/+}$ mice, which deacylate the LPS within 10 days of injection (Lu et al., 2008). In contrast, for at least 2–4 weeks after *Aoah*$^{-/-}$ mice receive a small intraperitoneal dose of LPS (10 μg), sufficient LPS remains to stimulate peritoneal macrophages to remain tolerant to LPS re-exposure (Lu et al., 2008, 2013).

Posokhova et al. found that an intraperitoneal dose of LPS induced peritoneal macrophages to increase neutral lipid synthesis for 18–24 h (Posokhova et al., 2008). To find out if prolonged LPS stimulation promotes neutral lipid accumulation for longer time periods, we first studied peritoneal macrophages from LPS-stimulated mice by staining the cells with Nile Red. Macrophages from *Aoah*$^{-/-}$ mice studied 14 days after an i.p. injection of LPS contained more neutral lipid than did macrophages from identically treated *Aoah*$^{+/+}$ mice. They accumulated even more lipid if the mice had been fed an high fat and high cholesterol (HFHC) diet (Spann et al., 2012; Que et al., 2018) (Figure 1A). We confirmed this result by staining macrophages with another neutral lipid dye, BODIPY, and analyzing them using flow cytometry (Figure 1B). When mice were fed either a regular diet or an HFHC diet, by 14 days after i.p. LPS injection, the *Aoah*$^{-/-}$ macrophages had accumulated more free cholesterol and cholesterol esters but less triglyceride than had *Aoah*$^{+/+}$ macrophages (Figure 1C). As expected, TLR4 was required to enhance cholesterol accumulation (Figures 1B and 1C). After 2 weeks on an HFHC diet with i.p. LPS injection on day 0, *Aoah*$^{-/-}$ and *Aoah*$^{+/+}$ mice had similar blood lipid levels (Figure S2), suggesting that cell-intrinsic changes in cholesterol metabolism are more important than blood cholesterol levels for increasing cholesterol accumulation in *Aoah*$^{-/-}$ macrophages.

### Cholesterol metabolism is dysregulated in LPS-exposed *Aoah*$^{-/-}$ macrophages

To explore how cholesterol accumulates in LPS-exposed *Aoah*$^{-/-}$ macrophages, we harvested peritoneal macrophages from *Aoah*$^{+/+}$ and *Aoah*$^{-/-}$ mice 21 days after i.p. LPS injection and performed microarrays (Lu et al., 2013). Using Kyoto Encyclopedia of Genes and Genomes (KEGG) pathway analysis, we found that the steroid biosynthesis pathway was upregulated in macrophages from *Aoah*$^{-/-}$ mice (data not shown). Further analysis revealed that the expression of genes for cholesterol uptake and biosynthesis increased, while the expression of cholesterol efflux genes decreased, in LPS-exposed *Aoah*$^{-/-}$ macrophages (Figure 2A, compare *Aoah*$^{+/+}$ and *Aoah*$^{-/-}$ groups). Notably, many of the gene expression changes in *Aoah*$^{-/-}$ macrophages were not present in *Aoah*$^{+/+}$ macrophages that had been re-treated with LPS for 2 h *ex vivo* (Figure 2A, compare the *Aoah*$^{+/+}$ and *Aoah*$^{+/+}$ LPS re-stimulation groups), suggesting that the gene expression changes caused by long-term LPS exposure may not be induced by acute LPS stimulation. Using qPCR and western blotting, we confirmed that *ApoE* expression diminished in tolerant *Aoah*$^{-/-}$ macrophages (Figures 2B and 2C), in keeping with previous findings that LPS stimulation decreases ApoE protein abundance (Thompson et al., 2010; Li et al., 2008). In contrast, tolerant *Aoah*$^{-/-}$ macrophages had decreased ABCA1 mRNA yet unchanged ABCA1 protein levels (Figures 2B and 2C). The low-density lipoprotein receptor (LDLR) expression significantly increased in tolerant *Aoah*$^{-/-}$ macrophages, as did the cells' ability to take up LDL, even when they were lipid laden (Figures 2B, 2D, and 2E). Taken together, these experiments revealed that AOAH plays an important role in preventing LPS-induced macrophage cholesterol accumulation. In contrast, the expression of genes involved in fatty acid uptake,

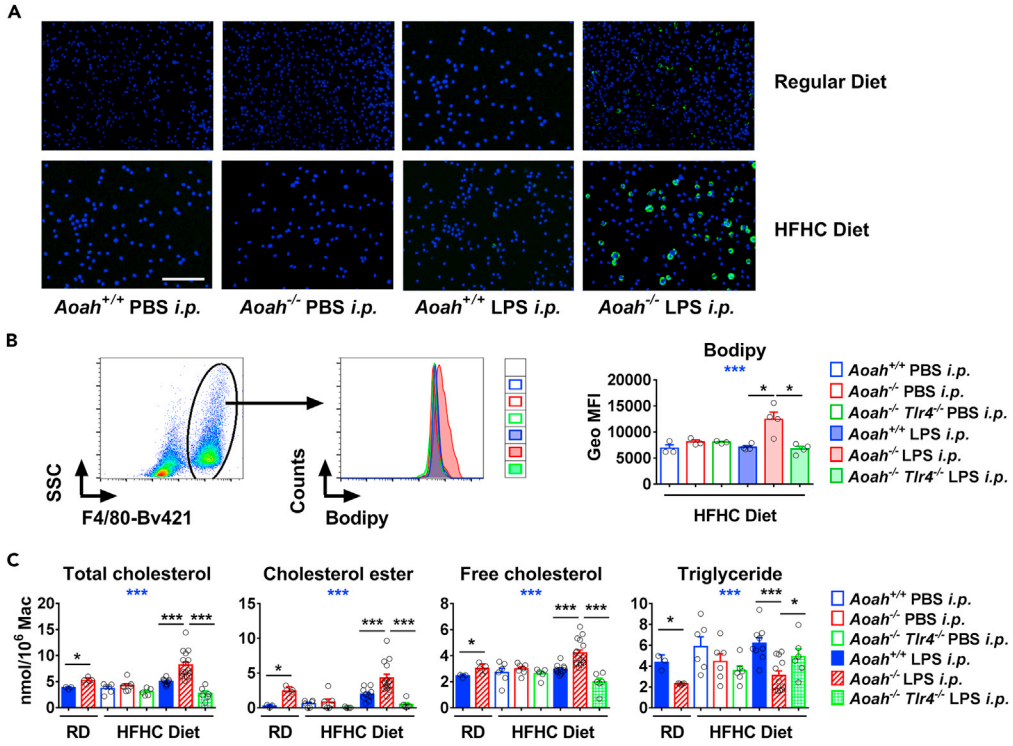


**Figure 1. LPS-exposed *Aoah*$^{-/-}$ peritoneal macrophages accumulate more cholesterol**

*Aoah*$^{+/+}$, *Aoah*$^{-/-}$, and *Aoah*$^{-/-}$*Tlr4*$^{-/-}$ mice were fed a regular diet (RD) or the HFHC diet. On day 0 they, were injected i.p. with either PBS or 10 μg LPS. On day 14, their peritoneal macrophages were studied.

(A) Macrophages were allowed to adhere to cell culture plates and stained with Nile Red. Similar results were observed in 4 experiments, n = 3 in each experiment. Scale bar represents 100 μm.

(B) Peritoneal cells were stained with anti-F4/80 antibody and BODIPY. The BODIPY fluorescence intensity of the F4/80$^{+}$ macrophages was measured using flow cytometry. n = 3 or 4.

(C) The amount of cholesterol and triglyceride was measured in adherent macrophages. Data were combined from at least 2 experiments, n ≥ 3/group.

Data were presented as mean ± SE. One-way analysis of variance (ANOVA) was used to test the 4 groups (blue stars), and the Mann-Whitney test was used to test difference between groups (black stars). *p < 0.05; **p < 0.01; ***p < 0.001.

See also Figures S1 and S2.

fatty acid biosynthesis, β-oxidation, and triacylglycerol metabolism did not show significant differences between LPS-exposed *Aoah*$^{+/+}$ and *Aoah*$^{-/-}$ macrophages (Figure S3). These results thus suggest that, after chronic LPS exposure *in vivo*, *Aoah*$^{-/-}$ peritoneal macrophages preferentially accumulate cholesterol rather than triglyceride (Huang et al., 2014b), in agreement with the biochemical findings (Figure 1C).

## After parenteral LPS exposure, *Aoah*$^{-/-}$ macrophages maintain unresolved inflammatory changes

As reported previously, sufficient stimulatory LPS persists in the peritoneal cavities of *Aoah*$^{-/-}$ mice 2–4 weeks after i.p. LPS injection to maintain endotoxin tolerance in peritoneal macrophages (Lu et al., 2013). This is evident from their diminished secretion, relative to *Aoah*$^{+/+}$ macrophages, of certain pro-inflammatory cytokines or chemokines (IL-6, TNF-α, RANTES), along with a normal IL-10 response, in response to re-stimulation with LPS *ex vivo* (Lu et al., 2008, 2013). To find out if the chronically stimulated *Aoah*$^{-/-}$ macrophages could nonetheless contribute to local or systemic inflammation, we again studied mice 14 days after i.p. LPS injection. *Aoah*$^{-/-}$ mice had elevated serum MCP-1 and RANTES (Figure 3A) and increased numbers of peritoneal macrophages, neutrophils, B and T lymphocytes, natural killer (NK) cells, and natural killer T (NKT) cells (Figure S4), indicating that some inflammatory responses had not resolved. In addition, analysis of microarray data from peritoneal macrophages harvested 21 days after LPS i.p. injection revealed increased expression of both pro- and anti-inflammatory mRNAs (TNF-α, IL-1β, IL-12α, and IL-10) in tolerant *Aoah*$^{-/-}$ mice (Figure 3B, compare *Aoah*$^{+/+}$ with *Aoah*$^{-/-}$). Using qPCR,

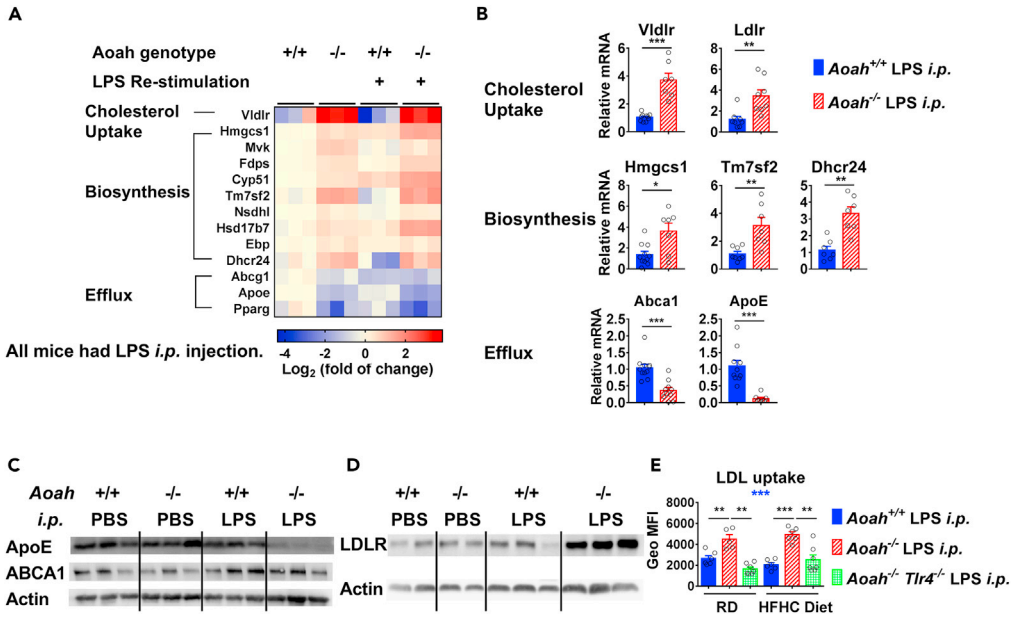


**Figure 2. LPS-exposed *Aoah*$^{-/-}$ peritoneal macrophages have dysregulated cholesterol metabolic gene expression (Next paragraph) Mice were injected i.p with 10 μg LPS**

(A) Twenty-one days later, their peritoneal macrophages were purified and cultured either untreated (*Aoah*$^{+/+}$, *Aoah*$^{-/-}$) or treated with 1 μg/mL LPS for 2 h *ex vivo* (*Aoah*$^{+/+}$ LPS, *Aoah*$^{-/-}$ LPS) before mRNA was collected for microarray analysis. The gene expression levels involved in cholesterol metabolism that were significantly different ($P < 0.05$) in *Aoah*$^{+/+}$ vs. *Aoah*$^{-/-}$ macrophages are shown. n = 3. The gene expression levels of *Aoah*$^{+/+}$ macrophages were set to 1, and the fold expression changes were calculated for the other groups.

(B–D) Fourteen days after LPS injection, peritoneal macrophages were purified, and qPCR analysis was performed (B). Data were combined from at least 2 experiments. n = 7–10. ApoE, ABCA1 (C), and LDLR (D) proteins in peritoneal macrophages were measured. n = 3. The western blots were repeated with similar results.

(E) Peritoneal cells were incubated with BODIPY-labeled LDL and then stained with anti-F4/80 antibody. LDL uptake by macrophages was measured using flow cytometry. n = 5–7.

Data were presented as mean ± SE. One-way ANOVA was used to test the 6 groups (blue stars), and the Mann-Whitney test was used to test difference between groups (black stars). *$p < 0.05$; **$p < 0.01$; ***$p < 0.001$.

See also Figure S3.

we confirmed that LPS-exposed *Aoah*$^{-/-}$ macrophages had increased expression of TNF-α, IL-1β, and IL-12α (Figure 3C), increased expression of an M1 marker gene, iNOS, and diminished expression of mRNAs for M2 markers Arg1, Fizz1, and Mrc1 (Figure 3D). In contrast, LPS-exposed *Aoah*$^{-/-}$ macrophages often had less robust responses to LPS re-stimulation *ex vivo* than did *Aoah*$^{+/+}$ macrophages (Figure 3B), in keeping with ongoing tolerance in the *Aoah*$^{-/-}$ cells. Taken together, these results suggest that while LPS-exposed *Aoah*$^{-/-}$ macrophages maintain "tolerance", in the sense that they are hypo-responsive to re-stimulation with LPS (Figure 3B) (Lu et al., 2008, 2013); they also increase production of some inflammatory mediators and do not transit to an M2 phenotype, maintaining features of unresolved inflammation (Tabas, 2010; Back et al., 2019).

## LPS-exposed *Aoah*$^{-/-}$ peritoneal macrophages have impaired mitochondria

As cholesterol efflux requires ATP, we next asked if LPS-exposed *Aoah*$^{-/-}$ macrophages had impaired energy metabolism (Karunakaran et al., 2015). First, we measured the accumulation of lactate in the culture medium and found that LPS-exposed *Aoah*$^{+/+}$ and *Aoah*$^{-/-}$ peritoneal macrophages had similar medium lactate levels. When *Aoah*$^{-/-}$ macrophages were re-stimulated with LPS *ex vivo*, however, they accumulated less medium lactate than did *Aoah*$^{+/+}$ macrophages, consistent with previous findings that tolerant monocytes/macrophages do not increase aerobic glycolysis upon innate stimulation (Figure 4A) (Lu et al., 2008, 2013; Cheng et al., 2016). We then stained macrophage mitochondria by infecting cells with an adenovirus that produces cytochrome *c* oxidase subunit 8a (Cox8a)-RFP (Jacobi et al., 2015). Compared with *Aoah*$^{+/+}$ macrophages, tolerant *Aoah*$^{-/-}$ peritoneal macrophages had shorter and more dispersed

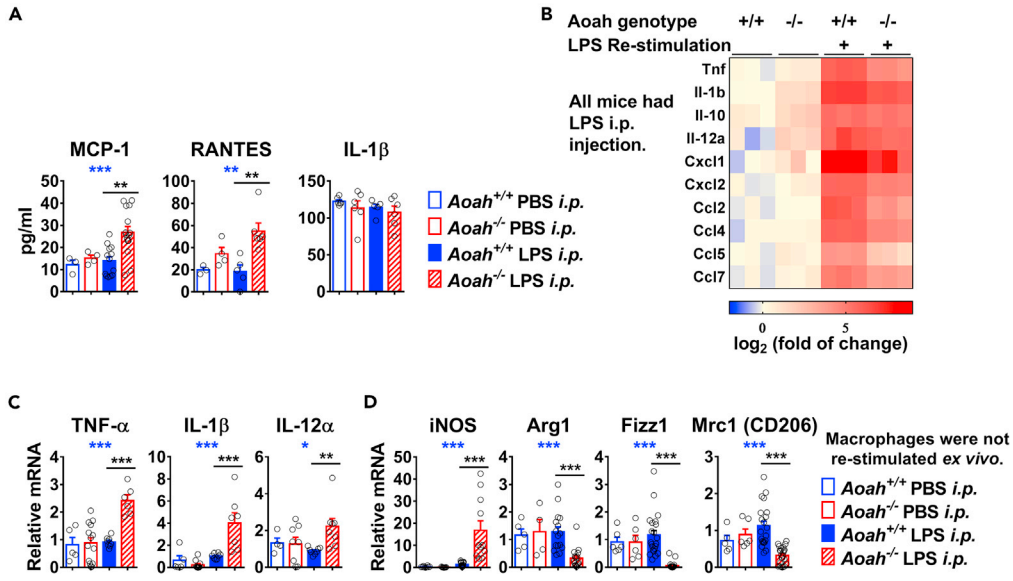


**Figure 3. After parenteral LPS exposure, *Aoah*$^{-/-}$ mice maintain residual inflammatory changes while *Aoah*$^{+/+}$ mice recover**

(A) Fourteen days after they received i.p. LPS injection, *Aoah*$^{-/-}$ mice had elevated serum chemokines MCP-1 and RANTES, n ≥ 3.

(B) Analysis of the same microarray data as in Figure 2A was performed, n = 3. The gene expression levels of *Aoah*$^{+/+}$ macrophages were set to equal 1, and fold expression changes were calculated for the other groups.

(C and D) Fourteen days after i.p. LPS, *Aoah*$^{-/-}$ peritoneal macrophages had increased expression of mRNAs for inflammatory genes (C); elevated M1 and decreased M2 marker expression (D). Data were combined from at least 2 experiments, n ≥ 4/group.

Data were presented as mean ± SE. One-way ANOVA was used to test the 4 groups (blue stars), and the Mann-Whitney test was used to test difference between groups (black stars). *p < 0.05; **p < 0.01; ***p < 0.001.

See also Figure S4.

mitochondria (Figure 4B). This result was confirmed when mitochondria were observed using electron microscopy (Figure 4C). Their cellular adenosine triphosphate (ATP) levels also were lower (Figure 4D). Flow cytometric analysis revealed that LPS-exposed *Aoah*$^{-/-}$ peritoneal macrophages had reduced mitochondrial mass (measured by MitoTracker Green staining), mitochondrial inner membrane potential (MitoTracker Red staining), and mitochondrial reactive oxygen species (ROS) (MitoSOX staining) (Figure 4E). In addition, we found that these macrophages had reduced expression of both mitochondrial biogenesis genes (Figure 4F) and genes encoding proteins involved in mitochondrial fusion and fission (Figure 4G). Collectively, these results indicate that LPS-exposed *Aoah*$^{-/-}$ macrophages have altered mitochondrial morphology and function that may contribute to defective cholesterol efflux by decreasing cellular ATP production.

## After parenteral exposure to LPS, AOAH prevents foam cell formation in carotid artery lesions

Having found that chronically LPS-exposed and HFHC-fed *Aoah*$^{-/-}$ mice develop cholesterol-laden, inflammatory macrophages, we asked if these mice were more likely to accumulate foam cells in their arteries than were *Aoah*$^{+/+}$ mice. Because LPS-induced changes in cholesterol uptake (increased LDLR) and efflux (decreased ApoE) play significant roles in promoting cholesterol accumulation in *Aoah*$^{-/-}$ macrophages, we chose an experimental model that does not require the absence of either of these genes. We followed the protocol published by Thusen et al. (von der Thusen et al., 2001), who found that the lesions that developed proximal to carotid artery collars included both neointimal (smooth muscle cell) and atheromatous (fat-laden macrophages) changes. We began feeding mice an HFHC diet, placed a silastic collar around the left carotid artery of each mouse one week later (von der Thusen et al., 2001), and injected a small dose (5 μg) of LPS or PBS intraperitoneally during weeks 2, 4, and 6 (Figure 5A). Two weeks after the last injection, we studied proximal carotid artery sections from each mouse and found that the arteries in

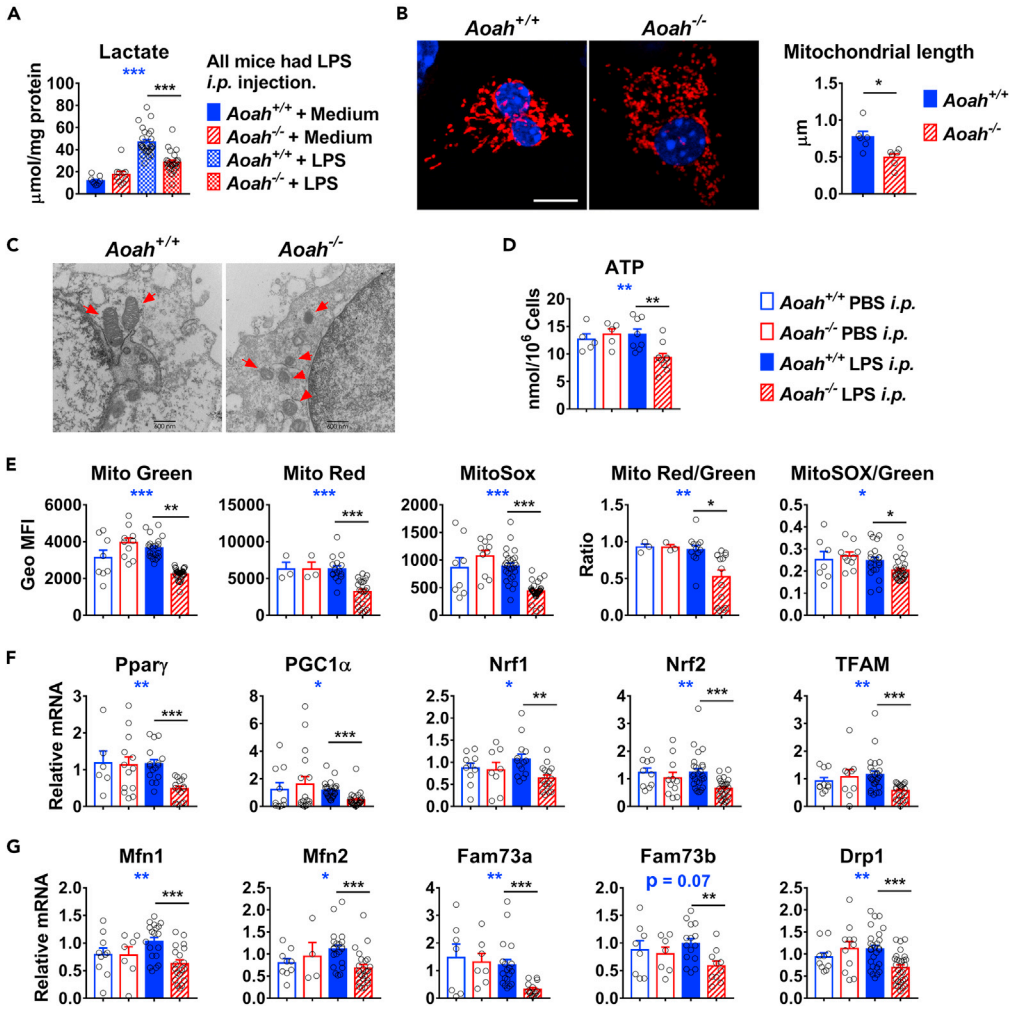


**Figure 4. LPS-exposed *Aoah*$^{-/-}$ peritoneal macrophages have impaired mitochondrial function**

*Aoah*$^{+/+}$ and *Aoah*$^{-/-}$ mice were injected i.p. with 10 μg LPS. Fourteen days later, their peritoneal macrophages were explanted.

(A) Peritoneal macrophages were treated with medium or 10 ng/mL LPS for 20 h. The medium lactate was measured. Data were combined from 3 experiments, n = 3 in each experiment.

(B) Peritoneal macrophages were stained with an adenovirus carrying Cox8a-RFP. Mitochondrial length was measured by using Image-Pro 6.0 Plus software. Approximately, 2000 mitochondrial lengths were measured in total 7 or 8 macrophages from 3 *Aoah*$^{-/-}$ or *Aoah*$^{+/+}$ mice, respectively. Scale bar represents 5 μm.

(C) Peritoneal macrophages were allowed to adhere and then fixed and processed for electron microscopy. Note that *Aoah*$^{-/-}$ macrophages had mitochondrial fragmentation and reduced cristae number. Representative pictures of total 9 macrophages from 3 mice of each genotype are shown. Arrows indicate mitochondria. Scale bar represents 600 nm. (D) Cellular ATP levels were measured. Data were combined from 2 experiments, each with n = 3.

(E) On day 14, mouse peritoneal macrophages were stained with MitoTracker Green (for measurement of mitochondrial mass), MitoTracker Red (mitochondrial inner membrane potential), and MitoSOX (mitochondrial ROS). The ratios of MitoTracker Red over MitoTracker Green and MitoSOX over MitoTracker Green were calculated. Data were combined from 2 experiments, each with n = 3 or 4.

(F) The expression of mitochondrial biogenesis genes was quantitated by using qPCR.

(G) The expression of mitochondrial fusion (Mfn1, Mfn2, Fam73a, and Fam73b) and fission (Drp1) genes was also measured. Data were combined from 3 experiments, each with n = 3 or 4.

Data were presented as mean ± SE. One-way ANOVA was used to test the 4 groups (blue stars), and the Mann-Whitney test was used to test difference between groups (black stars). *p < 0.05; **p < 0.01; ***p < 0.001.

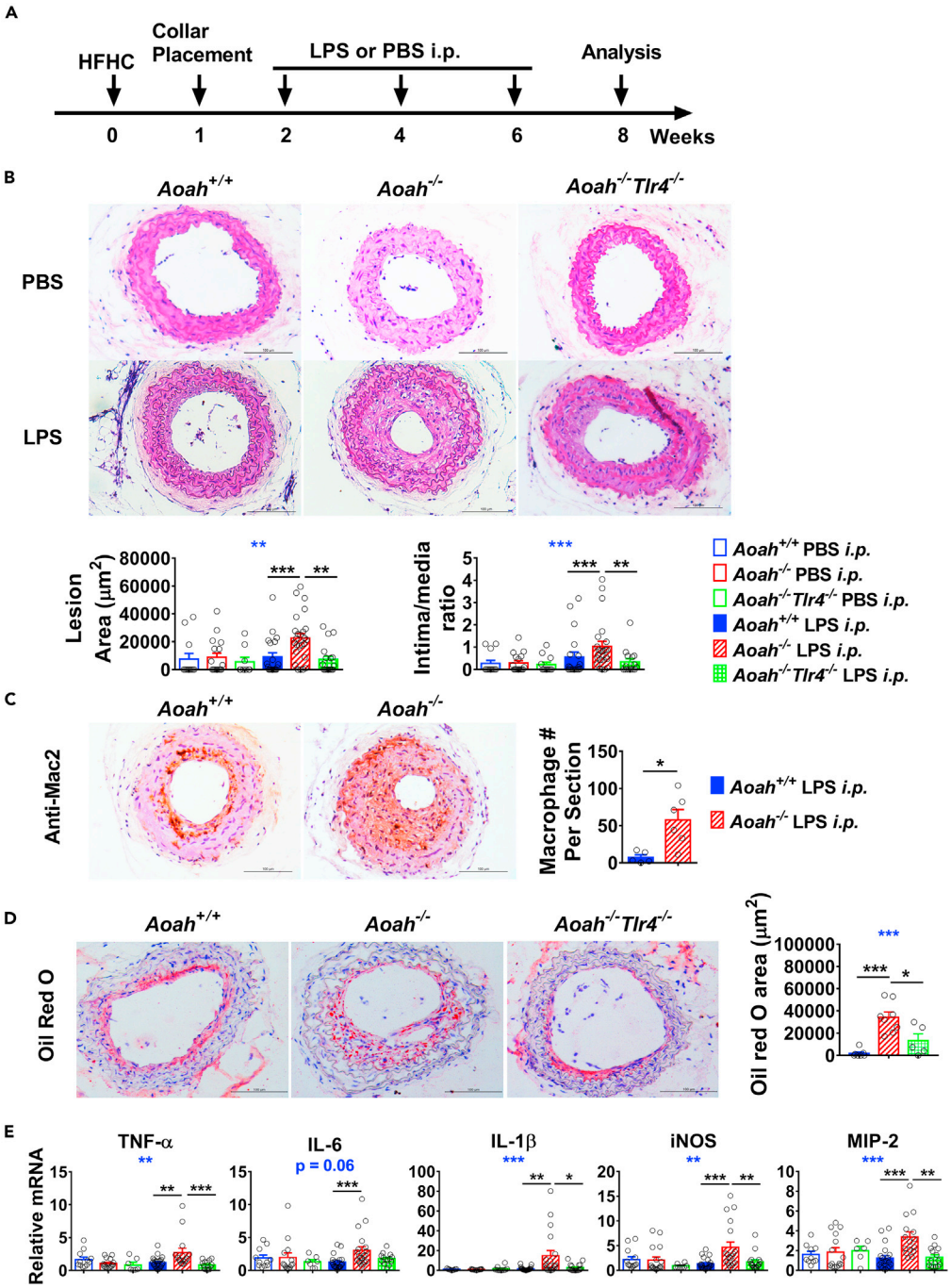


**Figure 5. After parenteral exposure to LPS, AOAH prevents foam cell formation in carotid artery lesions**

(A) Starting on day 0, mice were fed an HFHC diet. On day 7, a silastic collar was placed around the left carotid artery of each mouse. Mice were injected i.p. with PBS or 5 μg LPS on days 14, 28, and 42. They were euthanized on day 56 for analysis.

(B) The carotid artery segment proximal to the collar was obtained for histology. Hematoxylin- and eosin-stained cross sections are shown. The lesion areas were quantitated by using Image-Pro 6.0 Plus software. Data were combined from at least 4 experiments, n ≥ 8 mice/group.

(C) Cross sections were stained with anti-Mac2 antibody to visualize macrophages. n = 5 or 6 mice/group.

(D) After the carotid artery segment proximal to the collar was obtained, the segments were embedded in OCT and frozen at −80°C before they were sectioned for oil red O staining and quantitation. n ≥ 5 mice/group.

**Figure 5. *Continued***

(E) The intra-collar carotid segments, which also had plaques, were harvested and RNA was extracted for qPCR analysis. Data were combined from at least 3 experiments, n ≥ 9/group. Scale bars represent 100 μM (in B, C, D).

Data were presented as mean ± SE. One-way ANOVA was used to test the difference among 3 (D) or 6 (A, E) groups (blue stars), and the Mann-Whitney test was used to test difference between groups (black stars). *p < 0.05; **p < 0.01; ***p < 0.001.

See also Figure S5.

*Aoah*$^{-/-}$ mice that received i.p. LPS had developed a significant increase in intimal surface area (Figure 5B). The plaque was homogeneous, and the lesion area was much larger in *Aoah*$^{-/-}$ mice than in the *Aoah*$^{+/+}$ and *Aoah*$^{-/-}$*Tlr4*$^{-/-}$ controls (Figure 5B). Staining the tissue sections with anti-Mac2 antibody identified numerous macrophages in the plaques (Figure 5C), and oil red O staining showed that the macrophages were lipid laden (Figure 5D). We also stained the tissue sections for smooth muscle actin and found that the plaques in *Aoah*$^{-/-}$ mice that had received i.p. LPS injections contained few smooth muscle cells (data not shown). We next studied intra-collar carotid artery sections to measure the expression of pro-inflammatory molecules and found that the *Aoah*$^{-/-}$ lesions had significantly higher expression of mRNAs for TNF-α, IL-6, IL-1β, iNOS, and MIP-2 (Figure 5E). The increase in plaque size and inflammatory marker abundance observed in *Aoah*$^{-/-}$ mice was blunted in mice that lacked both AOAH and TLR4, confirming an essential pathogenetic role for LPS and possibly for LPS-induced molecules that stimulate TLR4 (Figures 5B, 5D, and 5E). In another experiment, we used AOAH transgenic mice that overproduce AOAH in macrophages (Ojogun et al., 2009) to test if AOAH is protective. After beginning the HFHC diet and placing collars, we injected LPS or PBS i.p. every other week for 5 times and analyzed mice two weeks after the last injection (Figure S5A, left panel). *Aoah*$^{Tg}$ mice had 24.6-fold higher AOAH mRNA in the intra-collar carotid segments than did *Aoah*$^{+/+}$ mice (Figure S5A, right panel, PBS groups). LPS i.p. injection increased AOAH expression in *Aoah*$^{+/+}$ and *Aoah*$^{Tg}$ mouse arteries by 3.0- and 3.7-fold, respectively (Figure S5A, right panel). The plaque size and carotid artery inflammation were significantly reduced in *Aoah*$^{Tg}$ mice (Figures S5B and S5C). Overproducing AOAH prevented foam cell accumulation in the arterial intima.

## DISCUSSION

In addition to the many studies that have supported the importance of MAMP recognition in host defense, recent reports have revealed an important role for host inactivation of MAMPs in preventing pulmonary fibrosis in mice (Van Dyken et al., 2017) and prolonging Lyme arthritis in humans (Jutras et al., 2019), as well as for modulating the abundance of stimulatory LPS in the mouse intestine and its translocation into the bloodstream (Qian et al., 2018; Han et al., 2021). Here, we present evidence that a key host mechanism for inactivating LPS can also prevent foam cell accumulation in a murine model of carotid atherosclerosis.

LPS-exposed *Aoah*$^{-/-}$ macrophages expressed significantly less ApoE and more LDLR and accumulated more cholesterol than did *Aoah*$^{+/+}$ macrophages, especially when mice were fed an HFHC diet. Cholesterol accumulation accompanied increased expression of genes that regulate cholesterol uptake and biosynthesis and decreased expression of cholesterol efflux genes. In addition, LPS-exposed *Aoah*$^{-/-}$ macrophages retained features of the M1 (classically activated) inflammatory phenotype.

Since LPS-exposed *Aoah*$^{-/-}$ macrophages had increased expression of *Ldlr* and decreased expression of *ApoE*, we reasoned that crossing the *Aoah*$^{-/-}$ mutation onto an *Ldlr*$^{-/-}$ or *ApoE*$^{-/-}$ background might obscure the impact of *Aoah* deficiency. We instead chose a perivascular carotid placement model (von der Thusen et al., 2001) that emphasizes both cholesterol accumulation and the role of abnormal blood flow and hemodynamics in pathogenesis. After they had received small LPS injections i.p. fortnightly for 6 weeks, *Aoah*$^{-/-}$ mice had more foam cells in their carotid arterial lesions than did *Aoah*$^{+/+}$ or *Aoah*$^{-/-}$*Tlr4*$^{-/-}$ mice, suggesting that LPS stimulation via TLR4 promoted foam cell accumulation. The lesions induced in LPS-injected *Aoah*$^{-/-}$ mice were similar to those reported for *Ldlr*$^{-/-}$ mice (von der Thusen et al., 2001). In addition, we found that mice that overexpressed AOAH in their macrophages were protected. These results provided strong evidence that AOAH can ameliorate foam cell accumulation *in vivo*.

Energy metabolism controls macrophage polarization and function (O'Neill et al., 2016; O'Neill and Pearce, 2016). Pro-inflammatory M1 macrophages use glycolysis to provide energy for innate immune responses while, during the resolution phase, M2 or alternatively activated macrophages depend more upon

mitochondrial oxidative phosphorylation to meet their energy needs (Mills and O'Neill, 2016; Galvan-Pena and O'Neill, 2014; Vats et al., 2006; Huang et al., 2014a). Failure to increase mitochondrial function inhibits the transition from M1 to M2 macrophages, preventing the resolution of inflammation and aggravating atherosclerosis (Van den Bossche et al., 2016; Ouimet et al., 2015; Karunakaran et al., 2015; Wei et al., 2018). We found that mitochondrial mass, inner membrane potential, and ROS decreased in tolerant *Aoah*$^{-/-}$ macrophages along with reduced cellular ATP levels, suggesting that mitochondrial function is not restored if LPS stimulation persists. LPS-exposed *Aoah*$^{-/-}$ macrophages consistently failed to convert from M1 to M2. Mitochondrial function also impacts cholesterol efflux, an ATP-dependent process (Allen et al., 2013; Karunakaran et al., 2015). Energy metabolism thus plays important roles in regulating both inflammation resolution and cholesterol metabolism in macrophages.

Collectively, our results show that a host lipase that inactivates a common bacterial MAMP, LPS, can prevent macrophage cholesterol accumulation (foam cell formation) and allow MAMP-promoted inflammatory changes to resolve. Others have found that other MAMPs (bacterial lipoproteins, flagellin, bacterial, or viral nucleic acids) can also induce foam cell/atheroma formation (Nicolaou et al., 2012; Angelovich et al., 2015); the results reported here raise the possibility that host-mediated inactivation of these MAMPs may also play a role in preventing this common pathological process.

### Limitations of the study

In this study, we show that prolonged exposure to LPS leads to unresolved inflammation, persistent tolerance, mitochondrial impairment, and cholesterol accumulation in macrophages that cannot inactivate LPS. How these features are related to each other awaits further investigation.

## STAR★METHODS

Detailed methods are provided in the online version of this paper and include the following:

- KEY RESOURCES TABLE
- RESOURCE AVAILABILITY
  - Lead contact
  - Materials availability
  - Data and code availability
- EXPERIMENTAL MODEL AND SUBJECT DETAILS
  - Mice
- METHOD DETAILS
  - Reagents
  - Flow cytometry
  - Macrophage lipid analysis
  - Blood lipid analysis
  - LDL uptake assay
  - LPS-induced inflammation
  - Quantitative PCR (qPCR) analysis
  - Western blotting analysis
  - Medium lactate assay
  - Transfer experiments
  - Mitochondrial analysis
  - Cellular ATP measurement
  - Induction of artery foam cell accumulation by perivascular carotid collar placement
- QUANTIFICATION AND STATISTICAL ANALYSIS

## SUPPLEMENTAL INFORMATION

Supplemental information can be found online at https://doi.org/10.1016/j.isci.2021.103004.

## ACKNOWLEDGMENTS

We thank Richard Kitchens (UT Southwestern Medical Center at Dallas) and Li-Hao Huang (Fudan University) for much helpful advice. This study was supported by grants 31770993, 91742104, and 31570910 from the National Natural Science Foundation of China (M.L.), grant 21ZR1405400 from the Shanghai Committee

of Science and Technology (M.L.), NIH grant RO1 AI18188 (R.S.M.), and by the Division of Intramural Research, National Institute for Allergy and Infectious Diseases, NIH, USA (R.S.M.).

## AUTHOR CONTRIBUTIONS

J.F., W.J., X.C., B.Z., A.W.V., T.L., G.Q., and M.L. designed and performed the experiments and analyzed the data. W.Z., J.T., Q.Z., Y.C., Y.W., and X.L. provided scientific advice. M.L. and R.S.M. designed the experiments, supervised the project and wrote the paper.

## DECLARATION OF INTERESTS

The authors declare no competing interests.

Received: June 1, 2021
Revised: July 14, 2021
Accepted: August 15, 2021
Published: September 24, 2021

## REFERENCES

Allen, A.M., Taylor, J.M., and Graham, A. (2013). Mitochondrial (dys)function and regulation of macrophage cholesterol efflux. Clin. Sci. (Lond). *124*, 509–515.

Angelovich, T.A., Hearps, A.C., and Jaworowski, A. (2015). Inflammation-induced foam cell formation in chronic inflammatory disease. Immunol. Cell Biol. *93*, 683–693.

Back, M., Yurdagul, A., Jr., Tabas, I., Oorni, K., and Kovanen, P.T. (2019). Inflammation and its resolution in atherosclerosis: mediators and therapeutic opportunities. Nat. Rev. Cardiol. *16*, 389–406.

Bjorkbacka, H., Kunjathoor, V.V., Moore, K.J., Koehn, S., Ordija, C.M., Lee, M.A., Means, T., Halmen, K., Luster, A.D., Golenbock, D.T., and Freeman, M.W. (2004). Reduced atherosclerosis in MyD88-null mice links elevated serum cholesterol levels to activation of innate immunity signaling pathways. Nat. Med. *10*, 416–421.

Carnevale, R., Nocella, C., Petrozza, V., Cammisotto, V., Pacini, L., Sorrentino, V., Martinelli, O., Irace, L., Sciarretta, S., Frati, G., et al. (2018). Localization of lipopolysaccharide from Escherichia Coli into human atherosclerotic plaque. Sci. Rep. *8*, 3598.

Cheng, S.C., Scicluna, B.P., Arts, R.J., Gresnigt, M.S., Lachmandas, E., Giamarellos-Bourboulis, E.J., Kox, M., Manjeri, G.R., Wagenaars, J.A., Cremer, O.L., et al. (2016). Broad defects in the energy metabolism of leukocytes underlie immunoparalysis in sepsis. Nat. Immunol. *17*, 406–413.

Curtiss, L.K., and Tobias, P.S. (2009). Emerging role of Toll-like receptors in atherosclerosis. J. Lipid Res. *50* (*Suppl*), S340–S345.

Galvan-Pena, S., and O'Neill, L.A. (2014). Metabolic reprograming in macrophage polarization. Front. Immunol. *5*, 420.

Geng, S., Chen, K., Yuan, R., Peng, L., Maitra, U., Diao, N., Chen, C., Zhang, Y., Hu, Y., Qi, C.F., et al. (2016). The persistence of low-grade inflammatory monocytes contributes to aggravated atherosclerosis. Nat. Commun. *7*, 13436.

Ghosn, E.E., Cassado, A.A., Govoni, G.R., Fukuhara, T., Yang, Y., Monack, D.M., Bortoluci, K.R., Almeida, S.R., Herzenberg, L.A., and Herzenberg, L.A. (2010). Two physically, functionally, and developmentally distinct peritoneal macrophage subsets. Proc. Natl. Acad. Sci. U S A *107*, 2568–2573.

Gioannini, T.L., Teghanemt, A., Zhang, D., Prohinar, P., Levis, E.N., Munford, R.S., and Weiss, J.P. (2007). Endotoxin-binding proteins modulate the susceptibility of bacterial endotoxin to deacylation by acyloxyacyl hydrolase. J. Biol. Chem. *282*, 7877–7884.

Gitlin, J.M., and Loftin, C.D. (2009). Cyclooxygenase-2 inhibition increases lipopolysaccharide-induced atherosclerosis in mice. Cardiovasc. Res. *81*, 400–407.

Han, Y.-H., Onufer, E.J., Huang, L.-H., Sprung, R.W., Davidson, W.S., Czepielewski, R.S., Wohltmann, M., Sorci-Thomas, M.G., Warner, B.W., and Randolph, G.J. (2021). Enterically derived high-density lipoprotein restrains liver injury through the portal vein. Science *373*, eabe6729.

Hsieh, W.Y., Zhou, Q.D., York, A.G., Williams, K.J., Scumpia, P.O., Kronenberger, E.B., Hoi, X.P., Su, B., Chi, X., Bui, V.L., et al. (2020). Toll-like receptors induce signal-specific reprogramming of the macrophage lipidome. Cell Metab. *32*, 128–143 e5.

Huang, S.C., Everts, B., Ivanova, Y., O'sullivan, D., Nascimento, M., Smith, A.M., Beatty, W., Love-Gregory, L., Lam, W.Y., O'neill, C.M., et al. (2014a). Cell-intrinsic lysosomal lipolysis is essential for alternative activation of macrophages. Nat. Immunol. *15*, 846–855.

Huang, Y.L., Morales-Rosado, J., Ray, J., Myers, T.G., Kho, T., Lu, M., and Munford, R.S. (2014b). Toll-like receptor agonists promote prolonged triglyceride storage in macrophages. J. Biol. Chem. *289*, 3001–3012.

Jacobi, D., Liu, S., Burkewitz, K., Kory, N., Knudsen, N.H., Alexander, R.K., Unluturk, U., Li, X., Kong, X., Hyde, A.L., et al. (2015). Hepatic Bmal1 regulates rhythmic mitochondrial dynamics and promotes metabolic fitness. Cell Metab. *22*, 709–720.

Jutras, B.L., Lochhead, R.B., Kloos, Z.A., Biboy, J., Strle, K., Booth, C.J., Govers, S.K., Gray, J., Schumann, P., Vollmer, W., et al. (2019). Borrelia burgdorferi peptidoglycan is a persistent antigen in patients with Lyme arthritis. Proc. Natl. Acad. Sci. U S A *116*, 13498–13507.

Karunakaran, D., Thrush, A.B., Nguyen, M.A., Richards, L., Geoffrion, M., Singaravelu, R., Ramphos, E., Shangari, P., Ouimet, M., Pezacki, J.P., et al. (2015). Macrophage mitochondrial energy status regulates cholesterol efflux and is enhanced by anti-miR33 in atherosclerosis. Circ. Res. *117*, 266–278.

Li, L., Thompson, P.A., and Kitchens, R.L. (2008). Infection induces a positive acute phase apolipoprotein E response from a negative acute phase gene: role of hepatic LDL receptors. J. Lipid Res. *49*, 1782–1793.

Lu, M., and Munford, R.S. (2011). The transport and inactivation kinetics of bacterial lipopolysaccharide influence its immunological potency in vivo. J. Immunol. *187*, 3314–3320.

Lu, M., Varley, A.W., and Munford, R.S. (2013). Persistently active microbial molecules prolong innate immune tolerance in vivo. PLoS Pathog. *9*, e1003339.

Lu, M., Varley, A.W., Ohta, S., Hardwick, J., and Munford, R.S. (2008). Host inactivation of bacterial lipopolysaccharide prevents prolonged tolerance following gram-negative bacterial infection. Cell Host Microbe *4*, 293–302.

Lu, M., Zhang, M., Takashima, A., Weiss, J., Apicella, M.A., Li, X.H., Yuan, D., and Munford, R.S. (2005). Lipopolysaccharide deacylation by an endogenous lipase controls innate antibody responses to Gram-negative bacteria. Nat. Immunol. *6*, 989–994.

Lu, Z., Li, Y., Brinson, C.W., Lopes-Virella, M.F., and Huang, Y. (2017). Cooperative stimulation of atherogenesis by lipopolysaccharide and palmitic acid-rich high fat diet in low-density lipoprotein receptor-deficient mice. Atherosclerosis *265*, 231–241.

Malik, T.H., Cortini, A., Carassiti, D., Boyle, J.J., Haskard, D.O., and Botto, M. (2010). The alternative pathway is critical for pathogenic complement activation in endotoxin- and diet-induced atherosclerosis in low-density lipoprotein receptor-deficient mice. Circulation *122*, 1948–1956.

Michelsen, K.S., Wong, M.H., Shah, P.K., Zhang, W., Yano, J., Doherty, T.M., Akira, S., Rajavashisth, T.B., and Arditi, M. (2004). Lack of Toll-like receptor 4 or myeloid differentiation factor 88 reduces atherosclerosis and alters plaque phenotype in mice deficient in apolipoprotein E. Proc. Natl. Acad. Sci. U S A *101*, 10679–10684.

Mills, E.L., and O'Neill, L.A. (2016). Reprogramming mitochondrial metabolism in macrophages as an anti-inflammatory signal. Eur. J. Immunol. *46*, 13–21.

Moore, K.J., Sheedy, F.J., and Fisher, E.A. (2013). Macrophages in atherosclerosis: a dynamic balance. Nat. Rev. Immunol. *13*, 709–721.

Munford, R.S., Weiss, J.P., and Lu, M. (2020). Biochemical Transformation of Bacterial Lipopolysaccharide by acyloxyacyl hydrolase reduces host injury and promotes recovery. J. Biol. Chem. *295*, 17842–17851.

Nicolaou, G., and Erridge, C. (2010). Toll-like receptor-dependent lipid body formation in macrophage foam cell formation. Curr. Opin. Lipidol. *21*, 427–433.

Nicolaou, G., Goodall, A.H., and Erridge, C. (2012). Diverse bacteria promote macrophage foam cell formation via Toll-like receptor-dependent lipid body biosynthesis. J. Atheroscler. Thromb. *19*, 137–148.

O'Neill, L.A., Kishton, R.J., and Rathmell, J. (2016). A guide to immunometabolism for immunologists. Nat. Rev. Immunol. *16*, 553–565.

O'Neill, L.A., and Pearce, E.J. (2016). Immunometabolism governs dendritic cell and macrophage function. J. Exp. Med. *213*, 15–23.

Ojogun, N., Kuang, T.Y., Shao, B., Greaves, D.R., Munford, R.S., and Varley, A.W. (2009). Overproduction of acyloxyacyl hydrolase by macrophages and dendritic cells prevents prolonged reactions to bacterial lipopolysaccharide in vivo. J. Infect. Dis. *200*, 1685–1693.

Ouimet, M., Ediriweera, H.N., Gundra, U.M., Sheedy, F.J., Ramkhelawon, B., Hutchison, S.B., Rinehold, K., Van Solingen, C., Fullerton, M.D., Cecchini, K., et al. (2015). MicroRNA-33-dependent regulation of macrophage metabolism directs immune cell polarization in atherosclerosis. J. Clin. Invest. *125*, 4334–4348.

Posokhova, E.N., Khoshchenko, O.M., Chasovskikh, M.I., Pivovarova, E.N., and Dushkin, M.I. (2008). Lipid synthesis in macrophages during inflammation in vivo: effect of agonists of peroxisome proliferator activated receptors alpha and gamma and of retinoid X receptors. Biochemistry (Mosc) *73*, 296–304.

Qian, G., Jiang, W., Zou, B., Feng, J., Cheng, X., Gu, J., Chu, T., Niu, C., He, R., Chu, Y., and Lu, M. (2018). LPS inactivation by a host lipase allows lung epithelial cell sensitization for allergic asthma. J. Exp. Med. *215*, 2397–2412.

Que, X., Hung, M.Y., Yeang, C., Gonen, A., Prohaska, T.A., Sun, X., Diehl, C., Maatta, A., Gaddis, D.E., Bowden, K., et al. (2018). Oxidized phospholipids are proinflammatory and proatherogenic in hypercholesterolaemic mice. Nature *558*, 301–306.

Spann, N.J., Garmire, L.X., Mcdonald, J.G., Myers, D.S., Milne, S.B., Shibata, N., Reichart, D., Fox, J.N., Shaked, I., Heudobler, D., et al. (2012). Regulated accumulation of desmosterol integrates macrophage lipid metabolism and inflammatory responses. Cell *151*, 138–152.

Stoll, L.L., Denning, G.M., and Weintraub, N.L. (2004). Potential role of endotoxin as a proinflammatory mediator of atherosclerosis. Arterioscler. Thromb. Vasc. Biol. *24*, 2227–2236.

Tabas, I. (2010). Macrophage death and defective inflammation resolution in atherosclerosis. Nat. Rev. Immunol. *10*, 36–46.

Thompson, P.A., Gauthier, K.C., Varley, A.W., and Kitchens, R.L. (2010). ABCA1 promotes the efflux of bacterial LPS from macrophages and accelerates recovery from LPS-induced tolerance. J. Lipid Res. *51*, 2672–2685.

Van den Bossche, J., Baardman, J., Otto, N.A., Van Der Velden, S., Neele, A.E., Van Den Berg, S.M., Luque-Martin, R., Chen, H.J., Boshuizen, M.C., Ahmed, M., et al. (2016). Mitochondrial dysfunction prevents repolarization of inflammatory macrophages. Cell Rep. *17*, 684–696.

Van Dyken, S.J., Liang, H.E., Naikawadi, R.P., Woodruff, P.G., Wolters, P.J., Erle, D.J., and Locksley, R.M. (2017). Spontaneous chitin accumulation in airways and age-related fibrotic lung disease. Cell *169*, 497–509 e13.

Vats, D., Mukundan, L., Odegaard, J.I., Zhang, L., Smith, K.L., Morel, C.R., Wagner, R.A., Greaves, D.R., Murray, P.J., and Chawla, A. (2006). Oxidative metabolism and PGC-1beta attenuate macrophage-mediated inflammation. Cell Metab. *4*, 13–24.

Vink, A., Schoneveld, A.H., Van Der Meer, J.J., Van Middelaar, B.J., Sluijter, J.P., Smeets, M.B., Quax, P.H., Lim, S.K., Borst, C., Pasterkamp, G., and De Kleijn, D.P. (2002). In vivo evidence for a role of toll-like receptor 4 in the development of intimal lesions. Circulation *106*, 1985–1990.

von der Thusen, J.H., Van Berkel, T.J., and Biessen, E.A. (2001). Induction of rapid atherogenesis by perivascular carotid collar placement in apolipoprotein E-deficient and low-density lipoprotein receptor-deficient mice. Circulation *103*, 1164–1170.

Wang, L., Beecham, A., Dueker, N., Blanton, S.H., Rundek, T., and Sacco, R.L. (2015). Sequencing of candidate genes in Dominican families implicates both rare exonic and common non-exonic variants for carotid intima-media thickness at bifurcation. Hum. Genet. *134*, 1127–1138.

Wei, Y., Corbalan-Campos, J., Gurung, R., Natarelli, L., Zhu, M., Exner, N., Erhard, F., Greulich, F., Geissler, C., Uhlenhaut, N.H., et al. (2018). Dicer in macrophages prevents atherosclerosis by promoting mitochondrial oxidative metabolism. Circulation *138*, 2007–2020.

Westerterp, M., Berbee, J.F., Pires, N.M., Van Mierlo, G.J., Kleemann, R., Romijn, J.A., Havekes, L.M., and Rensen, P.C. (2007). Apolipoprotein C-I is crucially involved in lipopolysaccharide-induced atherosclerosis development in apolipoprotein E-knockout mice. Circulation *116*, 2173–2181.

Wiedermann, C.J., Kiechl, S., Dunzendorfer, S., Schratzberger, P., Egger, G., Oberhollenzer, F., and Willeit, J. (1999). Association of endotoxemia with carotid atherosclerosis and cardiovascular disease: prospective results from the Bruneck Study. J. Am. Coll. Cardiol. *34*, 1975–1981.

Williams, J.W., Zaitsev, K., Kim, K.W., Ivanov, S., Saunders, B.T., Schrank, P.R., Kim, K., Elvington, A., Kim, S.H., Tucker, C.G., et al. (2020). Limited proliferation capacity of aortic intima resident macrophages requires monocyte recruitment for atherosclerotic plaque progression. Nat. Immunol. *21*, 1194–1204.

Zimmer, S., Grebe, A., and Latz, E. (2015). Danger signaling in atherosclerosis. Circ. Res. *116*, 323–340.

Zou, B., Jiang, W., Han, H., Li, J., Mao, W., Tang, Z., Yang, Q., Qian, G., Qian, J., Zeng, W., et al. (2017). Acyloxyacyl hydrolase promotes the resolution of lipopolysaccharide-induced acute lung injury. PLoS Pathog. *13*, e1006436.

## STAR★METHODS

### KEY RESOURCES TABLE

| REAGENT or RESOURCE | SOURCE | IDENTIFIER |
|---|---|---|
| Antibodies | | |
| Anti-mouse CD16/32 (clone 93) | Biolegend | Cat# 101302; RRID:AB_312801 |
| Anti-mouse F4/80-BV421 (clone BM8) | Biolegend | Cat# 123132; RRID:AB_11203717 |
| Anti-mouse B220-Percp-Cy5.5 (clone RA3-6B2) | Biolegend | Cat# 103236; RRID:AB_893354 |
| Anti-mouse Ly6G-FITC (clone 1A8) | BD | Cat# 551460; RRID:AB_394207 |
| Anti-mouse CD3-Alexa 647 (clone 17A2) | BD | Cat# 557869; RRID:AB_396912 |
| Anti-mouse NK1.1-PE (clone PK136) | BD | Cat# 553165; RRID:AB_394677 |
| Anti-mouse CD45.1-PerCP-Cy5.5 (clone A20) | BD | Cat# 560580; RRID:AB_1727489 |
| Anti-mouse CD45.2-APC (clone 104) | BD | Cat# 561875; RRID:AB_10896972 |
| Anti-Galectin 3 (Mac2) (clone A3A12) | Abcam | Cat# ab2785; RRID:AB_303298 |
| Anti-alpha smooth muscle actin | Abcam | Cat# ab5694; RRID:AB_2223021 |
| Anti-Apolipoprotein E Antibody (clone EPR19392) | Abcam | Cat# ab183597; RRID:AB_2832971 |
| Anti-ABCA1 Antibody (clone AB.H10) | Abcam | Cat# ab18180; RRID:AB_444302 |
| Mouse LDLR Antibody | R&D systems | Cat# AF2255; RRID:AB_355203 |
| HRP-Conjugated β Actin Monoclonal Antibody | Proteintech | Cat# HRP-66009; RRID:AB_2883836 |
| Bacterial and virus strains | | |
| Cox8a-RFP Adenovirus | Jacobi et al. (2015) | N/A |
| Biological samples | | |
| *Escherichia coli* 0111:B4 LPS | Sigma-Aldrich | Cat# L4130 |
| Chemicals, peptides, and recombinant proteins | | |
| Nile Red | Sigma-Aldrich | Cat# 19123 |
| Oil Red O | Sigma-Aldrich | Cat# O0625 |
| Bodipy FL LDL | Invitrogen | Cat# L3483 |
| MitoTracker Green | Invitrogen | Cat# M7514 |
| MitoTracker Red | Invitrogen | Cat# M22425 |
| MitoSox Red | Invitrogen | Cat# M36008 |
| DAPI | Beyotime Biotechnology | Cat# C1002 |
| RIPA Buffer | Beyotime Biotechnology | Cat# P0013B |
| PMSF | Beyotime Biotechnology | Cat# ST506 |
| Proteinase inhibitor cocktail | Sigma-Aldrich | Cat# P8340 |
| Fetal bovine serum | Gibco | Cat# 10099-141 |
| Molecular Probes™ ProLong™ Diamond Antifade Mountant | Thermo Fisher Scientific | Cat# P36970 |
| Immobilon Western HRP Substrate | Millipore | Cat# WBKLS0500 |
| Critical commercial assays | | |
| Triglyceride Quantification Assay Kit | Abcam | Cat# ab65336 |
| Cholesterol/Cholesteryl Ester Quantification Assay Kit | Abcam | Cat# ab65359 |
| Lactic Acid Assay Kit | Nanjing Jiancheng | Cat# A019-2-1 |
| CellTiter-Glo Luminescent Cell Viability Assay Kit | Promega | Cat# G7571 |
| Mouse MCP-1 ELISA Kit | BD | Cat# 555260 |
| Mouse RANTES ELISA Kit | R&D systems | Cat# DY478 |

(*Continued on next page*)

*Continued*

| REAGENT or RESOURCE | SOURCE | IDENTIFIER |
|---|---|---|
| Mouse IL-1β ELISA Kit | R&D systems | Cat# DY401 |
| RNA Isolation Kit | Tiangen | Cat# DP419 |
| First strand cDNA Synthesis Kit | Tiangen | Cat# KR116-02 |
| SYBR Green PCR Mixture | Tiangen | Cat# FP205-02 |
| **Deposited data** | | |
| Microarray data | Lu et al. (2013) | GEO:GSE40154 |
| **Experimental models: Organisms/strains** | | |
| Mouse: C57BL/6J | University of Texas Southwestern Medical Center | N/A |
| Mouse: C57BL/6J *Aoah*$^{-/-}$ | University of Texas Southwestern Medical Center | N/A |
| Mouse: C57BL/6J *Aoah*$^{-/-}$*Tlr4*$^{-/-}$ | University of Texas Southwestern Medical Center | N/A |
| Mouse: C57BL/6J *Aoah*$^{Tg}$ | University of Texas Southwestern Medical Center | N/A |
| **Oligonucleotides** | | |
| Primers for qPCR: AOAH Forward: GTTTTCCCAACGCTGCGGGG Reverse: TGGCCTTCTGCCCGGGTACA | This paper | N/A |
| Primers for qPCR: Abca1 Forward: CAGATGAAGCAGTTTTCAGTCCT Reverse: CACATTCCGGCTCTTTAGAAGG | This paper | N/A |
| Primers for qPCR: ApoE Forward: CTGACAGGATGCCTAGCCG Reverse: CGCAGGTAATCCCAGAAGC | This paper | N/A |
| Primers for qPCR: Vldlr Forward: AGACCAATCAGACGAGTCTCTT Reverse: CTGCCGTCCTTGCAGTCAG | This paper | N/A |
| Primers for qPCR: Ldlr Forward: TCCCTGGGAACAACTTCACC Reverse: CACTCTTGTCGAAGCAGTCAG | This paper | N/A |
| Primers for qPCR: Hmgcs1 Forward: AACTGGTGCAGAAATCTCTAGC Reverse: GGTTGAATAGCTCAGAACTAGCC | This paper | N/A |
| Primers for qPCR: Tm7sf2 Forward: GTCGCGGCTTTACTGATCCT Reverse: CAGGCAGATAGGCCGGTAG | This paper | N/A |
| Primers for qPCR: Dhcr24 Forward: CTCTGGGTGCGAGTGAAGG Reverse: TTCCCGGACCTGTTTCTGGAT | This paper | N/A |
| Primers for qPCR: TNF-α Forward: CATCTTCTCAAAATTCGAGTGACAA Reverse: TCAGCCACTCCAGCTGCTC | This paper | N/A |
| Primers for qPCR: IL-1b Forward: TGGGCCTCAAAGGAAAGAAT Reverse: CAGGCTTGTGCTCTGCTTGT | This paper | N/A |
| Primers for qPCR: IL-12a Forward: ATCTGGCGTCTACACTGCTG Reverse: TCTTCAGCAGGTTTCGGGAC | This paper | N/A |

(*Continued on next page*)

*Continued*

| REAGENT or RESOURCE | SOURCE | IDENTIFIER |
|---|---|---|
| Primers for qPCR: iNOS Forward: CTGCAGCACTTGGATCAGGAACCTG Reverse: GGGAGTAGCCTGTGTGCACCTGGAA | This paper | N/A |
| Primers for qPCR: Arg1 Forward: CAGAAGAATGGAAGAGTCAG Reverse: CAGATATGCAGGGAGTCACC | This paper | N/A |
| Primers for qPCR: Fizz1 Forward: TCCCAGTGAATACTGATGAGA Reverse: CCACTCTGGATCTCCCAAGA | This paper | N/A |
| Primers for qPCR: Mrc1 Forward: CTCTGTTCAGCTATTGGACGC Reverse: CGGAATTTCTGGGATTCAGCTTC | This paper | N/A |
| Primers for qPCR: IL-6 Forward: ATCGTGGAAATGAGAAAAGAGTTGT Reverse: TGGCCTTCTGCCCGGGTACA | This paper | N/A |
| Primers for qPCR: MIP-2 Forward: AGCTACATCCCACCCACACAG Reverse: AAAGCCATCCGACTGCATCT | This paper | N/A |
| Primers for qPCR: Actin Forward: GGCTGTATTCCCCTCCATCG Reverse: CCAGTTGGTAACAATGCCATGT | This paper | N/A |
| Software and algorithms | | |
| FlowJo (version 10) | Tree Star, Inc | https://www.flowjo.com/ |
| ImageJ | National Institutes of Health | https://imagej.nih.gov/ij/index.html |
| Image-Pro Plus 6.0 | Media Cybernetics, Inc | https://www.mediacy.com/imageproplus |
| Graphpad Prism (version 7) | GraphPad Software | https://www.graphpad.com/scientific-software/prism/ |
| Other | | |
| High fat high cholesterol (HFHC) diet | Research Diet | D12109C |

## RESOURCE AVAILABILITY

### Lead contact

Further information and requests for resources and reagents should be directed to the lead contact, Mingfang Lu (mingfanglu@fudan.edu.cn), Department of Immunology, School of Basic Medical Sciences, Fudan University, 138 Yixueyuan Road, PO Box 226, Xuhui District, Shanghai, China, 200032.

### Materials availability

The study did not generate new unique reagents.

### Data and code availability

The microarray data have been deposited in GEO (Gene Expression Omnibus) database supported by NCBI (GEO:GSE40154).

All datasets supporting the current study are available from the lead contact upon request.

## EXPERIMENTAL MODEL AND SUBJECT DETAILS

### Mice

C57BL/6J *Aoah*$^{+/+}$, *Aoah*$^{-/-}$, *Tlr4*$^{-/-}$ *Aoah*$^{-/-}$ and *Aoah*$^{Tg}$ mice were produced at the University of Texas Southwestern Medical Center, Dallas, Texas, transferred to the National Institutes of Health, Bethesda, Maryland,

and then provided to Fudan University, Shanghai. The mice were housed in specific pathogen-free conditions in the Department of Laboratory Animal Science, and studied using protocols approved by the Institutional Animal Care and Use Committee (IACUC) of Fudan University. All animal study protocols adhered to the Guide for the Care and Use of Laboratory Animals. Similar protocol and housing approval was in effect while the mice were in UT Southwestern Medical Center at Dallas and NIH. *Aoah*$^{+/+}$, *Aoah*$^{-/-}$, *Tlr4*$^{-/-}$*Aoah*$^{-/-}$ mice were co-housed for at least 3 weeks after they were weaned before experiments were started. Six - eight weeks old mice of both sexes were used, except that male mice were used for the perivascular carotid collar placement model as in previous studies (von der Thusen et al., 2001).

## METHOD DETAILS

### Reagents

*Escherichia coli* 0111:B4 LPS was obtained from Sigma. To test whether the LPS contained TLR agonists other than LPS, we compared the ability of LPS 0111 to stimulate *Tlr4*$^{+/+}$ and *Tlr4*$^{-/-}$ peritoneal macrophages. LPS 0111 was 200-fold more potent at inducing IL-6 secretion from *Tlr4*$^{+/+}$ peritoneal macrophages than from *Tlr4*$^{-/-}$ macrophages, suggesting that contamination with other TLR agonists was limited. The high fat high cholesterol (HFHC) diet (Research Diet, D12109C) contained protein: carbohydrate: fat (20:40:40, Calorie or 23:45:20, weight) as well as 1.25% cholesterol and 0.5% (w/w) sodium cholate.

### Flow cytometry

Peritoneal cells were harvested according to an online protocol https://bio-protocol.org/e976. The cells were incubated on ice with Fc-blocker (Anti-Mouse CD16/32, BioLegend. 1:200 dilution) for 30 min. Anti-mouse F4/80 Ab-Bv421 (BM8, BioLegend), anti-Ly6G Ab-FITC (1A8, BD), anti-CD3 Ab-Alexa 647 (17A2, BD), Anti-B220 Ab-Percp-Cy5.5 (RA3-6B2, BD), Anti-NK1.1 Ab-PE (PK136, BD) were added. All antibodies were used at 1:200 dilution. After 30 min incubation on ice, cells were washed with PBS twice and subjected to flow cytometric analysis (BD Celesta). Flowjo software was used to analyze data. Dead cells were excluded based on FSC and SSC gating.

### Macrophage lipid analysis

Co-housed *Aoah*$^{+/+}$, *Aoah*$^{-/-}$ and *Aoah*$^{-/-}$*Tlr4*$^{-/-}$ mice on a regular diet or a HFHC diet were injected i.p. with 10 μg LPS on days 0. On day 14, mice were euthanized by cervical dislocation, their peritoneal cells were flushed using 5 ml PBS and peritoneal macrophages were purified by allowing them to adhere to culture dishes (Lu et al., 2013).

Nile Red staining. Adherent peritoneal macrophages were fixed with 4% paraformaldehyde for 30 min at 25°C. Nile Red diluted in saline (5 μg/ml) was added to cell culture plates. After incubation for 1 h, the cells were washed and 0.3 μM DAPI (Beyotime Biotechnology) was added to stain nuclei. After washing, Molecular Probes™ ProLong™ Diamond Antifade Mountant (Thermo Fisher Scientific) was added. The cells were examined by using a fluorescence microscope (Leica, DMI4000B).

*Bodipy staining.* Peritoneal cells were incubated on ice with Fc-blocker (BD) for 30 min. Anti-mouse F4/80-Bv421 Ab and 2 μM Bodipy were added. After 30 min additional incubation, macrophage (F4/80$^{+}$) -associated Bodipy fluorescence was measured using FACS.

*Cholesterol and triglyceride analysis.* To measure cholesterol, peritoneal macrophages were resuspended in 200 μl chloroform: Isopropanol: NP-40 (7:11:0.1). After centrifugation, the organic (liquid) phase containing cholesterol was isolated and organic solvent was evaporated. The extracted cholesterol was measured according to the manufacturer's protocol (Abcam). To measure triglyceride, 5% NP-40/dd$H_2O$ solution was added. The samples were heated at 80-100°C for 5 min, centrifuged to remove insoluble material and measured according to the manufacturer's protocol (Abcam).

### Blood lipid analysis

Total cholesterol, LDL, HDL and triglyceride in mouse serum samples were determined by Shanghai Laboratory Animal Research Centre Sino-British SIPPR/B&K Lab Animal Ltd.

### LDL uptake assay

Peritoneal macrophages were cultured in RPMI medium containing 0.3% BSA (no serum) and incubated with 5 μg/ml BODIPY-labeled native LDL (Thermo Fisher Scientific) at 37°C for 4 h. Cell-associated BODIPY fluorescence was analyzed using flow cytometry.

### LPS-induced inflammation

Co-housed *Aoah*$^{+/+}$ and *Aoah*$^{-/-}$ mice were injected with 10 μg LPS or PBS i.p. Fourteen days later, their peritoneal cells were obtained and cultured in RPMI 1640 containing 10% fetal bovine serum, 100 U/ml penicillin, 0.1 mg/ml streptomycin and 2 mM L-glutamine (Gibco). The macrophages were purified by adherence to culture plates before they were lysed for microarray or qPCR. The methods for the microarray experiment and analysis have been published (Lu et al., 2013). *Aoah*$^{+/+}$ and *Aoah*$^{-/-}$ mice were injected i.p with 10 μg LPS. Twenty-one days later, their peritoneal macrophages were collected, purified and cultured either untreated (*Aoah*$^{+/+}$, *Aoah*$^{-/-}$) or treated with 1 μg/ml LPS for 2 h (*Aoah*$^{+/+}$ LPS, *Aoah*$^{-/-}$ LPS) before mRNA was collected for microarray analysis (Illumina MouseWG-6_v1_1 arrays). The microarray data have been deposited in GEO (Gene Expression Omnibus) database supported by NCBI (GSE40154). Data were analyzed using Illumina's GenomeStudio v2010.1 software.

### Quantitative PCR (qPCR) analysis

Total RNA from macrophages or blood vessels was isolated using a RNA isolation kit (Tiangen) and then mRNA was reverse-transcribed using a first strand cDNA synthesis kit (Tiangen). Quantitative PCR was performed on a LightCycler 480 II Instrument (Roche) using SYBR Green PCR mixture (Tiangen). Actin was used as the internal control and the relative mRNA abundance was calculated using the ΔΔCt quantification method.

### Western blotting analysis

Adherent peritoneal macrophages were lysed using RIPA buffer (Biyuntian) containing 1 mM PMSF (Biyuntian) and proteinase inhibitor cocktail (Sigma). Immobilon Western HRP substrate (Millipore) was used to detect proteins in Western blotting and the blot bands were quantified by using ImageJ.

### Medium lactate assay

Peritoneal macrophages were cultured in RPMI 1640 containing 1% fetal bovine serum with 10 ng/ml LPS or not for 20 h, and the medium lactate concentration was measured using a lactic acid assay kit (Nanjing Jiancheng Bioengineering Institute) following the manufacturer's protocol.

### Transfer experiments

Donor *Aoah*$^{+/+}$ and *Aoah*$^{-/-}$ CD45.1 mice were euthanized and their peritoneal cells were harvested. Approximately 2 X $10^6$ *Aoah*$^{+/+}$ or *Aoah*$^{-/-}$ cells were injected i.p to each *Aoah*$^{+/+}$ or *Aoah*$^{-/-}$ CD45.2 recipient mouse. Twenty-four hours after transfer, half of the recipient mice of either genotype received 1 μg *E. coli* 014 LPS i.p. Fourteen days later, recipient mice were euthanized and their peritoneal cells were harvested and subjected to FACS analysis. F4/80+ cells were identified as peritoneal macrophages. Then the donor and recipient macrophages were separated by using anti-CD45.1 Ab-PerCP-Cy5.5 (Clone A20, BD) or anti-CD45.2 Ab-APC (Clone 104, BD) and the frequency of donor and recipient macrophages was obtained. As monocytes were recruited following i.p. LPS injection, the donor macrophages were diluted. Based on the factor of dilution, we could calculate the frequency of monocyte-derived macrophages [monocyte-derived Mac / (Recipient Mac + Donor Mac + Monocyte-derived Mac)] in the peritoneal macrophage population.

### Mitochondrial analysis

*Laser scanning confocal microscopy.* Peritoneal macrophages were allowed to adhere to cover slips. Adenoviruses carrying Cox8a-RFP ($10^{10}$ virus/ml) were added to culture medium (Jacobi et al., 2015). After 24 hrs, the cells were washed and fixed using 4% paraformaldehyde. After 30 min incubation at 25°C, 0.3 μM DAPI was added to stain the nuclei. The samples were examined on a Leica SP6 confocal microscope. Mitochondrial length was measured blindly by using the Image-Pro 6.0 Plus software.

*Transmission electron microscopy.* Peritoneal macrophages were purified by adherence. 2.5% glutaraldehyde (2.5%) was added to the cell culture medium (1: 15, v/v). The cells were scraped, transferred to a 1.5 ml tube, and centrifuged at 2000 x g for 5 mins. The cell pellet was re-suspended in 2.5% glutaraldehyde at 4°C for 18 hrs before being processed for transmission electron microscopy at Shanghai Veterinary Research Institute. The samples were examined with a FEI Tecnai Spirit T12 transmission electron microscope at 80 kV.

*Mitochondrial staining and analysis.* Peritoneal cells were harvested and treated with Fc blocker on ice for 30 mins. The cells were then stained with anti-mouse F4/80 Ab, 100 nM MitoTracker Green, 100 nM MitoTracker Red or 5 μM MitoSOX for 30 mins at 37°C before flow cytometric analysis.

### Cellular ATP measurement

To measure cellular ATP levels, after the cells were washed with PBS and CellTiter-Glo Reagent (Promega) was added. After 10 min incubation, the luminescence was read (Tecan).

### Induction of artery foam cell accumulation by perivascular carotid collar placement

A described carotid collar placement method was used with modifications (von der Thusen et al., 2001). Co-housed *Aoah*$^{+/+}$, *Aoah*$^{-/-}$ and *Aoah*$^{-/-}$*Tlr4*$^{-/-}$ male mice were fed the HFHC diet starting on day 0. On day 7, perivascular collars (Dow Corning, inside diameter = 0.30 ± 0.08 mm, outside diameter = 0.64 ± 0.08 mm, wall = 0.15 mm) were placed around the left carotid artery as previously described (von der Thusen et al., 2001). On days 14, 28 and 42, mice were injected i.p. with 5 μg LPS in 200 μl PBS or an equal volume of PBS. On day 56 the mice were euthanized and perfused with PBS for 15 min and then with 4% formalin for 30 min. Their carotid arteries were then dissected. The proximal segments, which were close to the common carotid artery and not covered by the silastic collar, were fixed with 4% paraformaldehyde. We cut 30 sections of each sample and used #10, #20 and #30 sections for Hematoxylin & Eosin staining, immunochemistry (Mac2 staining), and quantitation. The average values of the 3 sections was used for each mouse. For Oil red O staining, the proximal carotids were embedded in OCT compound, frozen in -80°C before cutting. The intra-collar segments were dissected and put in RNA later for qPCR. To compare *Aoah*$^{+/+}$ and *Aoah*$^{Tg}$ mice, after collar placement, mice were injected with 5 μg LPS every two weeks for 5 times and analyzed two weeks after the last injection.

Hematoxylin- & eosin-stained sections were used for morphometric analysis. Quantitative analysis of lesions was performed with Image-Pro 6.0 Plus software. The intimal surface area was calculated by subtracting the lumen area from the area circumscribed by the internal elastic lamina. The medial surface area was defined as the area between the internal elastic lamina and the external elastic lamina. The intima/media ratio was determined by dividing the intimal area by the medial area.

## QUANTIFICATION AND STATISTICAL ANALYSIS

All values were expressed as mean ± SEM. One-Way ANOVA was used to test the experiments with more than two groups. Differences between groups were further analyzed by the Mann-Whitney U tests (unpaired, two-tailed test). All statistical analysis was performed with Graphpad Prism 7. *, $p < 0.05$; **, $p < 0.01$; ***, $p < 0.001$.